



X International Conference on Structural Dynamics, EURODYN 2017

Damage Detection in Structures Based on Principal Component Analysis of Forced Harmonic Responses

Jean-Claude Golinval^a

^aUniversity of Liege, Department of Aerospace and Mechanical Engineering, LTAS-Vibrations et Identification des Structures, Quartier Polytech 1, 9 Allée de la Découverte (B52/3), 4000 Liège, Belgium

Abstract

An approach based on principal component analysis (PCA) is considered here to tackle the problem of structural damage detection. The key idea of PCA is to reduce a large number of measured data to a much smaller number of uncorrelated variables while retaining as much as possible of the variation in the original data. PCA is applied here to the problem of damage detection in structures submitted to harmonic excitation. When processing vibration measurements, it can be shown that the basis of eigenvectors (called the proper orthogonal modes) span the same subspace as the mode-shape vectors of the monitored structure. Thus the damage detection problem may be solved using the concept of subspace angle between a reference subspace spanned by the eigenvectors of the initial (undamaged) structure and the subspace spanned by the eigenvectors of the current (possibly damaged) structure. The method is illustrated on the example of a real truss structure for damage detection and is combined to a model updating technique for damage localization.

© 2017 The Authors. Published by Elsevier Ltd.
Peer-review under responsibility of the organizing committee of EURODYN 2017.

Keywords: Damage detection; Principal component analysis; Harmonic excitation; ; Damage localization.

1. Introduction

The damage detection method considered here is based on principal component analysis (PCA) of the time responses of a structure. The objective is to show that, if the system is forced by an harmonic excitation, the number of proper orthogonal modes is restricted to two modes which can be used for damage detection as well as for damage localization when a structural model is available. PCA is also known as proper orthogonal decomposition (POD) and started to be used in the middle of the 20th century with the appearance of powerful computers. Its first applications in the field of structural dynamics date back to the 1990s. For an historical perspective on PCA (POD), the reader is referred to reference [1]. The use of PCA for structural health monitoring described here originates from the works presented in references [2] and [3]. It has been successfully applied for operational modal analysis (OMA) of civil

* Corresponding author. Tel.: +32-4-366-9177.
E-mail address: JC.Golinval@ulg.ac.be

engineering structures including temperature effects [4]. In this paper, we consider the case of damage detection in structures using harmonic excitation. First, the definition of PCA and its interpretation in the case of forced harmonic excitation are briefly recalled. Then a damage indicator based on angles between subspaces and a localization indicator based on residual strain energy are considered. Finally, the PCA based- procedure of structural damage detection is illustrated on the real example of a laboratory truss structure.

2. Principal Component Analysis

2.1. Definition and mathematical formulation

PCA is a multi-variate statistical method that aims at obtaining a compact representation of measured data. Its detailed mathematical formulation can be found in references [1] and [5] and consists in representing a zero mean random field $\theta(x, t)$ as

$$\theta(x, t) = \sum_{i=1}^{\infty} a_i(t) \phi_i(x) \quad (1)$$

where x and t are the continuous space and time variables respectively; $a_i(t)$ are uncorrelated coefficients and the orthogonal eigenfunctions $\phi_i(x)$ define the proper orthogonal modes (POMs). Each POM is associated to a proper orthogonal value (POV) which amplitude measures the energy percentage captured by the considered POM with respect to the total energy contained in the data and defined by the sum of the POVs.

2.2. Computation of the POMs

In practice, the data are discretized in space and time. Accordingly, the measured displacements at m locations on the structure and at n different time instants are collected in the $(m \times n)$ response matrix \mathbf{Q} as follows

$$\mathbf{Q} = [\mathbf{q}(t_1) \ \mathbf{q}(t_2) \ \dots \ \mathbf{q}(t_n)] = \begin{bmatrix} q_1(t_1) & q_1(t_2) & \dots & q_1(t_n) \\ \dots & \dots & \dots & \dots \\ q_m(t_1) & q_m(t_2) & \dots & q_m(t_n) \end{bmatrix} \quad (2)$$

It is demonstrated in reference [5] that the POMs and POVs correspond to the eigensolutions of the sample covariance matrix defined by

$$\mathbf{\Sigma} = \frac{1}{n} \mathbf{Q} \mathbf{Q}^T \quad (3)$$

It is also shown that the POMs and POVs result from the singular value decomposition (SVD) of the response matrix:

$$\mathbf{Q} = \mathbf{U} \mathbf{S} \mathbf{V}^T \quad (4)$$

where \mathbf{U} is an $(m \times m)$ orthonormal matrix, the columns of which being the POMs; \mathbf{S} is an $(m \times n)$ pseudo-diagonal and semi-positive definite matrix with diagonal entries containing the singular values; the POVs correspond to the square of the singular values divided by the number of samples m ; \mathbf{V} is an $(n \times n)$ orthonormal matrix, the columns \mathbf{v}_i of which containing the time modulation of the corresponding POM \mathbf{u}_i , normalized by the singular value σ_i .

One important property of the POMs is that they are optimal with respect to the energy content of the responses in a least squares sense as they capture more energy per mode than any other set of basis functions [1].

2.3. Interpretation of the POMs

In the case of an undamped and unforced linear system, it has been demonstrated in [6] that the POMs converge to the eigenmodes of the system when the mass matrix is proportional to identity if a sufficient number of samples is considered.

Let us consider here the case of a damped system submitted to harmonic excitation. The equation of motion may be written as follows:

$$\mathbf{M} \ddot{\mathbf{q}} + \mathbf{C} \dot{\mathbf{q}} + \mathbf{K} \mathbf{q} = \mathbf{F} \sin(\omega t) \tag{5}$$

where \mathbf{M} , \mathbf{C} and \mathbf{K} are the mass, damping and stiffness matrices, respectively; \mathbf{q} is the vector of displacement coordinates, \mathbf{F} is the vector of harmonic force of constant amplitude and ω is the excitation frequency. The forced response is synchronous to the excitation and may be written in the form

$$\mathbf{q}(t) = \Im \left(\mathbf{q}_f e^{i \omega t} \right) \tag{6}$$

where \mathbf{q}_f is the complex vector of forced response amplitudes and $\Im(\cdot)$ stands for the imaginary part.

The complex vector of forced response amplitude is given by

$$\mathbf{q}_f = \left(\mathbf{K} - \omega^2 \mathbf{M} + i \omega \mathbf{C} \right)^{-1} \mathbf{F} = \mathbf{H}(i \omega) \mathbf{F} \tag{7}$$

where $\mathbf{H}(i \omega)$ defines the matrix of frequency response functions (FRFs). It follows that the forced response writes

$$\begin{aligned} \mathbf{q}(t) &= \Im \left(\mathbf{H}(i \omega) \mathbf{F} e^{i \omega t} \right) \\ &= \Im \{ (\Re(\mathbf{H}) + i \Im(\mathbf{H})) (\mathbf{F} \cos(\omega t) + i \mathbf{F} \sin(\omega t)) \} \\ &= \Re(\mathbf{H}) \mathbf{F} \sin(\omega t) + \Im(\mathbf{H}) \mathbf{F} \cos(\omega t) \end{aligned} \tag{8}$$

The $(m \times n)$ response matrix \mathbf{Q} becomes

$$\begin{aligned} \mathbf{Q} &= [\mathbf{q}(t_1) \dots \dots \mathbf{q}(t_n)] \\ &= [\Re(\mathbf{H}) \mathbf{F} \sin(\omega t_1) + \Im(\mathbf{H}) \mathbf{F} \cos(\omega t_1) \quad \dots \quad \Re(\mathbf{H}) \mathbf{F} \sin(\omega t_n) + \Im(\mathbf{H}) \mathbf{F} \cos(\omega t_n)] \end{aligned} \tag{9}$$

Equation (9) may be expressed in the form

$$\begin{aligned} \mathbf{Q} &= \Re(\mathbf{H}) \mathbf{F} \begin{bmatrix} \sin(\omega t_1) \\ \vdots \\ \sin(\omega t_n) \end{bmatrix}^T + \Im(\mathbf{H}) \mathbf{F} \begin{bmatrix} \cos(\omega t_1) \\ \vdots \\ \cos(\omega t_n) \end{bmatrix}^T = \Re(\mathbf{H}) \mathbf{F} \mathbf{e}_s^T + \Im(\mathbf{H}) \mathbf{F} \mathbf{e}_c^T \\ &= \left[\Re(\mathbf{H}) \mathbf{F} \quad \Im(\mathbf{H}) \mathbf{F} \quad \mathbf{A} \right] \begin{bmatrix} 1 & 0 & 0 & \dots & 0 \\ 0 & 1 & 0 & \dots & 0 \\ 0 & 0 & 0 & \dots & 0 \\ \vdots & \vdots & \vdots & \ddots & \vdots \\ 0 & 0 & 0 & \dots & 0 \end{bmatrix} \left[\mathbf{e}_s \quad \mathbf{e}_c \quad \mathbf{B} \right]^T \\ &= \left[\frac{\Re(\mathbf{H}) \mathbf{F}}{\|\Re(\mathbf{H}) \mathbf{F}\|} \quad \frac{\Im(\mathbf{H}) \mathbf{F}}{\|\Im(\mathbf{H}) \mathbf{F}\|} \quad \mathbf{A} \right] \begin{bmatrix} \|\Re(\mathbf{H}) \mathbf{F}\| \|\mathbf{e}_s\| & 0 & 0 & \dots & 0 \\ 0 & \|\Im(\mathbf{H}) \mathbf{F}\| \|\mathbf{e}_c\| & 0 & \dots & 0 \\ 0 & 0 & 0 & \dots & 0 \\ \vdots & \vdots & \vdots & \ddots & \vdots \\ 0 & 0 & 0 & \dots & 0 \end{bmatrix} \left[\frac{\mathbf{e}_s}{\|\mathbf{e}_s\|} \quad \frac{\mathbf{e}_c}{\|\mathbf{e}_c\|} \quad \mathbf{B} \right]^T \\ &= \underbrace{\left[\frac{\Re(\mathbf{H}) \mathbf{F}}{\|\Re(\mathbf{H}) \mathbf{F}\|} \quad \frac{\Im(\mathbf{H}) \mathbf{F}}{\|\Im(\mathbf{H}) \mathbf{F}\|} \quad \mathbf{A} \right]}_{\mathbf{U}} \underbrace{\begin{bmatrix} \mathbf{I}_1 \end{bmatrix}}_{\mathbf{S}} \underbrace{\left[\frac{\mathbf{e}_s}{\|\mathbf{e}_s\|} \quad \frac{\mathbf{e}_c}{\|\mathbf{e}_c\|} \quad \mathbf{B} \right]^T}_{\mathbf{V}^T} \end{aligned} \tag{10}$$

where \mathbf{A} is an $(m \times (m - 2))$ matrix, \mathbf{I}_1 is an $(m \times n)$ matrix containing two non-zero elements $\|\Re(\mathbf{H}) \mathbf{F}\| \|\mathbf{e}_s\|$ and $\|\Im(\mathbf{H}) \mathbf{F}\| \|\mathbf{e}_c\|$, and \mathbf{B} is an $(n \times (n - 2))$ matrix. Matrices \mathbf{A} and \mathbf{B} do not influence equation (10) since they are both

multiplied by zero elements. If \mathbf{A} and \mathbf{B} are chosen in order that \mathbf{U} and \mathbf{V} are unitary matrices, then equation (10) is the singular value decomposition of matrix \mathbf{Q} . In conclusion, the following points may be noted.

1. Since there is only two non-zero singular values, the forced harmonic response of the system is captured by two POMs whatever the number of measurement co-ordinates is.
2. With the assumption of proportional damping, the FRF matrix takes the form

$$\mathbf{H}(i\omega) = \sum_{k=1}^m \frac{1}{\mu_k} \frac{\boldsymbol{\psi}_{(k)} \boldsymbol{\psi}_{(k)}^T}{\omega_k^2 - \omega^2 + 2i\zeta_k \omega \omega_k} \quad (11)$$

where ω_k is the k^{th} natural frequency, $\boldsymbol{\psi}_{(k)}$ is the k^{th} eigenvector, ζ_k is the modal damping and μ_k the modal mass. Thus analytic expressions of the POMs are obtained:

$$\mathbf{u}_{(1)} = \frac{\sum_{k=1}^m (\omega_k^2 - \omega^2) \boldsymbol{\psi}_{(k)} \boldsymbol{\psi}_{(k)}^T \mathbf{F} / (\mu_k ((\omega_k^2 - \omega^2)^2 + 4\zeta_k^2 \omega^2 \omega_k^2))}{\|\sum_{k=1}^m (\omega_k^2 - \omega^2) \boldsymbol{\psi}_{(k)} \boldsymbol{\psi}_{(k)}^T \mathbf{F} / (\mu_k ((\omega_k^2 - \omega^2)^2 + 4\zeta_k^2 \omega^2 \omega_k^2))\|} \quad (12)$$

$$\mathbf{u}_{(2)} = -\frac{\sum_{k=1}^m 2\zeta_k \omega \omega_k \boldsymbol{\psi}_{(k)} \boldsymbol{\psi}_{(k)}^T \mathbf{F} / (\mu_k ((\omega_k^2 - \omega^2)^2 + 4\zeta_k^2 \omega^2 \omega_k^2))}{\|\sum_{k=1}^m 2\zeta_k \omega \omega_k \boldsymbol{\psi}_{(k)} \boldsymbol{\psi}_{(k)}^T \mathbf{F} / (\mu_k ((\omega_k^2 - \omega^2)^2 + 4\zeta_k^2 \omega^2 \omega_k^2))\|} \quad (13)$$

3. It can be noted that both POMs ($\mathbf{u}_{(1)}$ and $\mathbf{u}_{(2)}$) reflect the real and imaginary parts, respectively, of the forced vibration mode commonly known as the operating deflection shape (ODS).
4. The POMs appear as a combination of all the eigenmodes. However, when the excitation frequency ω is close to one of the system's natural frequencies, the first POM will tend to the shape of the nearby mode.
5. In the absence of damping ($\mathbf{C} = \mathbf{0}$), the imaginary part of the FRF matrix ($\Im(\mathbf{H})$) is equal to zero and one single POM exists, which confirms the theory presented in reference [1].

2.4. Detection of damage using the concept of angles between subspaces

Detection of damage is performed here using the concept of subspace angles introduced in reference [2]. If \mathbf{U}_h and \mathbf{U}_d define the matrices of POMs corresponding to the healthy structure and the damaged structure respectively, their QR factorization allows computing orthonormal bases such that:

$$\mathbf{U}_h = \mathbf{Q}_h \mathbf{R}_h \quad (14)$$

$$\mathbf{U}_d = \mathbf{Q}_d^T \mathbf{R}_d \quad (15)$$

By definition [7], the singular values of $\mathbf{Q}_h \mathbf{Q}_d$ define the cosines of the principal angles θ_i between the subspaces \mathbf{Q}_h and \mathbf{Q}_d . These angles, and specifically the largest one, quantify how the subspaces \mathbf{Q}_h and \mathbf{Q}_d are globally different.

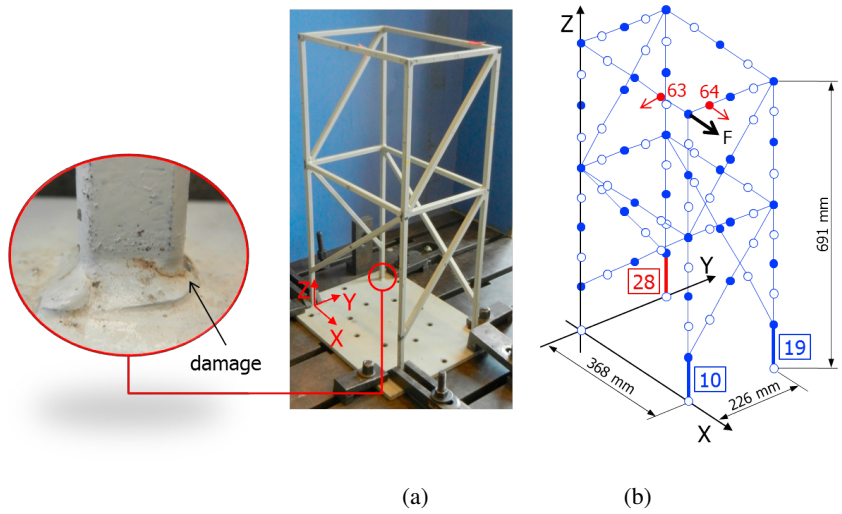
When harmonic excitation is considered, equations (12) and (13) show that the POMs span a two dimensional subspace which is representative of the state of the structure as the subspace depends on all the modal parameters of the structure (natural frequencies, damping ratios and mode-shapes).

2.5. Localization of damage using the concept of strain energy functions

As the POMs may be interpreted as displacement vectors forming a basis which allows to reconstruct the responses in an optimal way, they can be used for comparison between different states of the structure. Damage localization is based here on the calculation of strain energy functions based upon the elementary stiffness matrices of the FE model [8][9]. For the j^{th} element or substructure, it can be expressed as

$$\Delta E_{(k)}^j = (\mathbf{u}_{d,(k)}^j - \mathbf{u}_{h,(k)}^j)^T \mathbf{K}^j (\mathbf{u}_{d,(k)}^j - \mathbf{u}_{h,(k)}^j) \quad k = 1, 2 \quad (16)$$

where $\mathbf{u}_{d,(k)}^j$ represents the components of the "displacement" vector associated to the j^{th} element or substructure and corresponding to the k^{th} POM of the damaged structure and $\mathbf{u}_{h,(k)}^j$ is the equivalent vector for the healthy structure.



Legend: ● location of measurement DOFs

Fig. 1. (a) Truss structure; (b) FE model.

3. Example of a truss structure

3.1. Description of the truss structure

The application example considered here consists of a real truss structure made of steel and clamped at its base as illustrated in Figure 1(a). It was built in 1992 for testing modal identification techniques of structures submitted to base excitation on electrodynamic shaker [10]. The finite element (FE) model of the reference (undamaged) structure is shown in Figure 1(b). It is made of 92 Euler beam elements of hollow square cross-section (12 × 12 mm, thickness 1.4 mm) and totalizes 492 degrees of freedom.

Experimental modal analysis (EMA) was performed in the frequency range from 0 to 400 Hz with a frequency resolution of 0.1 Hz using impact excitation. A set of 56 measurements on each face of the truss at each corner and in the middle of each beam in the direction perpendicular to the face (directions X or Y) was measured by the technique of the roving hammer for two reference accelerometers located at nodes 63 (Y) and 64 (X) respectively. The results of modal identification obtained by the PolyMax method [11] are reported in Table 1 in terms of natural frequencies and damping ratios for the 9 first modes and compared with the FE results and with the results obtained in 1992 [10].

Table 1. Natural frequencies and damping ratios of the truss structure.

Mode	FE results Natural frequency (Hz)	EMA results (1996) Natural frequency (Hz)	EMA results (1996) damping ratio (%)	EMA results (2016) Natural frequency (Hz)	EMA results (2016) Damping ratio (%)
1	78.21	77.3	1.1	77.72	0.0266
2	124.59	126.5	3.3	108.99	0.4506
3	137.66	137.4	1.4	134.59	0.0634
4	160.19	158.5	0.5	158.91	0.1261
5	190.69	184.5	1.3	184.63	0.0572
6	208.76	207.5	0.8	209.36	0.0267
7	243.74	243.2	1.2	246.03	0.0112
8	256.42	255.5	0.9	260.24	0.2406
9	331.54	292.8	1.9	295.29	0.0239

The 2016 EMA reveals the apparition of a damage located at one of the feet of the truss structure and caused by rust as it can be observed in the inset picture of Figure 1. It was assessed that this damage can be simulated by a reduction of stiffness of 40% of element n° 28 (see Figure 1(b)).

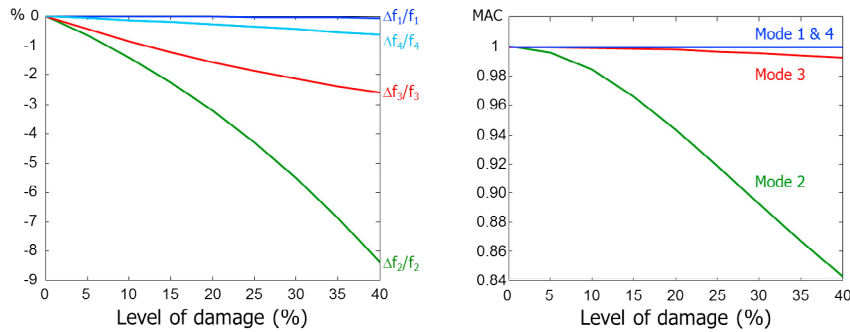


Fig. 2. (a) Relative error on natural frequencies; (b) Evolution of MAC

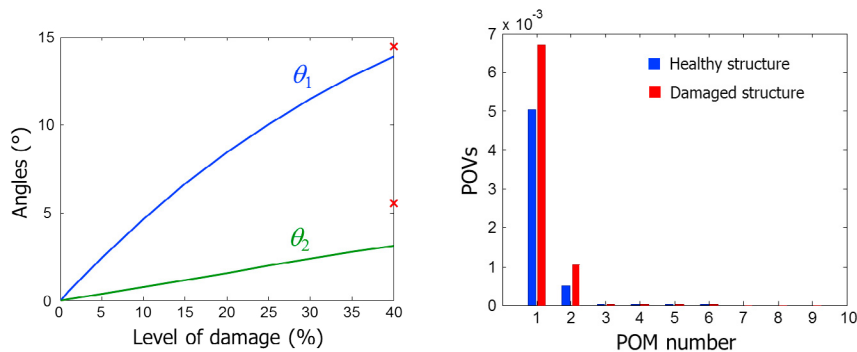


Fig. 3. (a) Damage detection using the subspace angles indicator; (b) Proper orthogonal values (POVs)

3.2. PCA analysis of forced harmonic responses

In order to illustrate the damage detection technique proposed in this paper, nine levels of stiffness reduction of element $n^\circ 28$ are considered: 1, 5, 10, 15, 20, 25, 30, 35 and 40 % respectively. The evolution of the relative error on the natural frequencies and of the modal assurance criterion (MAC)) with respect to damage is shown in Figures 2(a) and (b). It can be observed that modes 2 and 3 are the most affected by the presence of the damage.

In the following, the truss is supposed to be excited at one of its upper corners by a harmonic force F of 1 N acting in direction X at a frequency of 130 Hz as shown in Figure 1(b); the time-responses are computed for the different levels of damage using the damping ratios recorded in 1992 on the healthy structure. A last computation is also performed on the actual damaged truss (40 % stiffness reduction in element $n^\circ 28$) using the current damping ratios (EMA performed in 2016). The results of damage detection using the subspace angle indicator described in section 2.4 are given in Figure 3(a). In this figure, the red crosses correspond to the angles obtained with the experimental damping ratios of the current damaged truss. As expected, it shows that the indicator (specifically the first angle) is sensitive to a modification of the natural frequencies and mode-shapes and thus is able to detect damage. The detection is even more obvious if the actual damping level is considered. This result comes from the analytic expressions (12) and (13) of the POMs which show their sensitivity to all the modal parameters (natural frequencies, mode-shapes and damping ratios). Note also that similar results are obtained for different forcing frequencies.

As predicted, the PCA analysis of the time-responses reveals the presence of two POMs (Figure 3(b)). These POMs can be used for damage localization as explained in section 2.5 using the indicator based on strain energy functions. The results are given in Figure 4. Note that, as residual deformations are distributed over the structure, the strain energy indicator shows scattered residual energies. In this case, the result reveals that damage is located in element $n^\circ 28$ but also shows the presence of errors in elements $n^\circ 10$ and 19 which correspond to the elements clamped at the base. This confirms that methods of damage localization should be applied with care and that engineering insight is always necessary to assess the likely damages.

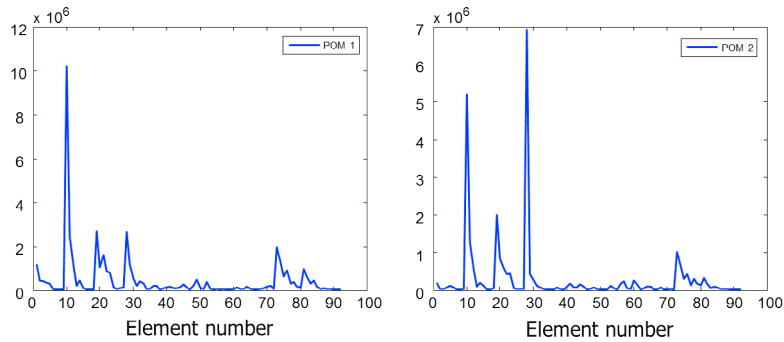


Fig. 4. Damage localization based on strain energy functions.

4. Conclusion

A damage detection method based on PCA has been considered in the case of harmonically excited structures. One advantage of the method is that it does not require modal identification (EMA) as it is directly based on the processing of time-responses. Another advantage is that the damage indicator based on the concept of subspace angles is a global indicator including all the modal information of the structure. Consequently, it does not require to select modes that are sensitive to damage as it would be the case in EMA. As the POMs obtained from PCA of the responses are scaled by the excitation force and may be interpreted as deformation vectors, they can be used for damage localization when a reliable FE model is available.

References

- [1] G. Kerschen, J.-C. Golinval, A. Vakakis, L. Bergman, The method of proper orthogonal decomposition for dynamical characterization and order reduction of mechanical systems: an overview, *Nonlinear Dynamics* (2005) 41: 147–169.
- [2] P. De Boe, J.-C. Golinval, Principal component analysis of piezo-sensor array for damage localization, *Structural Health Monitoring* 2 (2) (2003), 137–144.
- [3] A.-M. Yan, G. Kerschen, P. De Boe, J.-C. Golinval, Structural damage diagnosis under varying environmental conditions - Part I: A linear analysis, *Mechanical Systems & Signal Processing*, Academic Press Ltd Elsevier Science Ltd, (2005) 19(4), 847–864.
- [4] V.H. Nguyen, J. Mahowald, J.-C. Golinval, S. Maas, Damage Detection in Civil Engineering Structure Considering Temperature Effect, *International Modal Analysis Conference (IMAC) XXXII*, Society of Experimental Mechanics, Orlando (FL), 3-6 February 2014.
- [5] P. Holmes, J. Lumley, G. Berkooz, *Turbulence, coherent structures, Dynamical systems and symmetry*, Cambridge, New York, 1996.
- [6] G. Kerschen, J.-C. Golinval, Physical interpretation of the proper orthogonal modes using the singular value decomposition, *Journal of Sound and Vibration* (2002) 249(5), 849–865.
- [7] G. Golub, C. Van Loan, *Matrix computations*, The Johns Hopkins University Press, Baltimore, 1996.
- [8] M. Friswell, J. Motterhead, *Finite element model updating in structural dynamics*, Kluwer Academic Publishers, 1995.
- [9] P. Collignon, J.-C. Golinval, Finite element model updating and failure detection based on constitutive equation errors, *2nd International Conference in Structural Dynamics and Modelling: Test, Analysis, Correlation & Updating*, Proceedings of the DTA/NAFEMS conference, Lake Windermere, Cumbria, U.K., 3-5 July 1996, 307–317.
- [10] M. Razeto, *Identification de paramètres en dynamique des structures. Application à des problèmes non traditionnels*, Ph.D. thesis, Collection des publications de la Faculté des Sciences Appliquées n° 150, Université de Liège, 1996.
- [11] B. Peeters, H. Van Der Auweraer, P. Guillaume, J. Leuridan, The PolyMAX frequency-domain method: a new standard for modal parameter estimation?, *Shock and Vibration*, (3-4), 395409, 2004.